Eur. Phys. J. B **8**, 125–135 (1999)

THE EUROPEAN PHYSICAL JOURNAL B

EDP Sciences

Influence of the surface deformability and variable viscosity on buoyant – thermocapillary instability in a liquid layer

Zh. Kozhoukharova[1,a] and C. Rozé[2,b]

[1] Institute of Mechanics, 4, Acad. G. Bonchev Str., 1113 Sofia, Bulgaria
[2] LESP[c], CNRS-INSA et Université de Rouen, B.P. 8, 76131 Mont-Saint-Aignan Cedex, France

Received 15 May 1997

Abstract. The primary stationary and oscillatory Bénard-Marangoni instability is investigated in a fluid layer of infinite horizontal extent, bounded below by a rigid plane and above by a deformable upper surface, subjected to a vertical temperature gradient. Since the viscosity is temperature-dependent the consequences of relaxing Oberbeck-Boussinesq approximation and free surface deformability are theoretically examined by means of small disturbance analysis. The problem has been solved numerically by the Taylor series expansion method. The results obtained confirm that when the free surface is undeformable, stationary convection develops in the form of polygonal cells, and oscillatory motion cannot be detected. When the surface deformability is considered, stationary convection sets in, either as a short-wavelength hexagonal instability or as a long-wavelengh mode or as both, and oscillatory convection is also possible. The stability threshold for the short-wavelength mode depends mainly on the viscosity variation while the long-wavelength mode is determined by the surface deformation. Numerically, it is found that the neutral oscillatory Marangoni numbers are only negative. When a variable-viscosity model is used the theoretical and experimental results are in better agreement.

PACS. 47.20.-k Hydrodynamic stability – 47.27.-i Turbulent flows, convection, and heat transfer – 68.10.-m Fluid surfaces and fluid-fluid interfaces

1 Introduction

The Bénard-Marangoni instability induced by buoyancy forces within the volume and/or by surface-tension-gradients along the upper free surface of a liquid layer has received considerable attention. This phenomenon arises whenever the temperature gradient across the layer exceeds a certain critical value. Substantial progress regarding the thermal instability has been made since the experiments performed by Bénard. Applying the methods of the linear perturbation technique for predicting the appearance of thermal instability leads us back to the original theoretical analysis of Rayleigh. While Pearson's theoretical work [1] explained the thermocapillary instability mechanism, Nield [2] considered coupled buoyant and thermocapillary mechanism.

Even though many authors have treated the problem experimentally and theoretically there remain discrepancies between measured [3–6] and theoretically determined instability thresholds. The values available from Koschmieder and Switzer's experiment [3] are below those predicted from Nield's theoretical approach, in which the surface is supposed flat. Nitschke and Thess [4] reported the observed critical temperature difference to coincide with the predicted one. While the critical Marangoni number (the main relevant parameter of the instability) measured by Schatz *et al.* [5] agrees with theory, the experiments [6] found the onset of the instability in very thin liquid layers to occur 35% below the predictions of linear stability analysis. This experiment is concerned with the long-wavelength instability originating from the fluctuations of the free surface height, while the Schatz's *et al.* [5] ones are related to the short-wavelength hexagonal instability due to the temperature fluctuations on the free surface. Theoretically it is predicted [7–14] that the long-wavelength mode becomes more important for very thin and viscous liquid layers and, in microgravity, and can even set in as a primary instability.

Another hypothesis of Nield's model is that the transport coefficients are assumed to be relatively insensitive to temperature variations. For some liquids, however, the dynamic viscosity varies significantly with the temperature, an effect that cannot always be neglected. A variable viscosity was introduced by Palm and starting with his work [15] most investigations (see, for example, [16–18]) have been restricted to Rayleigh-Bénard buoyancy instability problems.

[a] e-mail: zhkozh@imbm.acad.bg
[b] e-mail: Claude.Roze@coria.fr
[c] UMR 6614

Recently, several works have been devoted to the problem of interaction between surface-tension and variable viscosity effects. The only observations of the flow patterns caused by the temperature differences across the layer with a free surface have been performed by Hoard *et al.* [19] and the critical Marangoni numbers were not reported. First, Lebon and collaborators [20,21] theoretically studied the coupled effects of a variable viscosity and a deformable upper surface on the onset of pure stationary thermocapillary convection. This analysis has been extended in two different ways. While in [22,23] the coupled effects of buoyancy and thermocapillarity were considered, but under the hypothesis that the upper boundary remains flat, in [24] the gravity waves as well as a temperature-dependent viscosity on the free surface were taken into account. A problem of stationary Marangoni instability in a flat liquid layer has been treated by Slavtchev and Ouzounov [25] under the exponential law of viscosity dependance on temperature, and in microgravity.

The aim of this article is twofold. First, it provides a development of the study by Gouesbet *et al.* [13] concerning a variable viscosity effect and secondly, it generalizes the study of Selak and Lebon [22] considering free surface deformability. The main problems in question are to determine the influence of these two factors on the convective threshold and to show a better agreement between the theory and experimental data.

2 Formulation of the problem

2.1 Mathematical model

The primary stationary and oscillatory instabilities in a liquid layer initially at rest and stimulated by heating from below or above are studied. The Fourier law of heat conduction is taken for granted. The liquid layer is assumed to be of infinite horizontal extent confined between a rigid plane $z = 0$ and a free surface with thickness d. Cartesian coordinates are used: two horizontal axes $\mathbf{x}$ and $\mathbf{y}$ are located at the rigid wall and a positive axis $\mathbf{z}$ is directed toward the free surface.

The fluid is supposed to have Newtonian density

$$\rho = \rho_0 \left[1 - \alpha \left(T - T_0\right)\right], \tag{1}$$

where T is the temperature of the liquid, ρ_0 is its value at a reference temperature T_0 and α is the positive coefficient of the thermal liquid expansion.

It is a reasonable approximation for a wide variety of liquids [20–25] to extend the Boussinesq model and consider also the kinematic viscosity to be temperature dependent. Here, a linear law for the kinematic viscosity is selected

$$\nu = \nu_0 + \zeta \left(T - T_0\right), \tag{2}$$

where ν_0 is viscosity at the reference temperature T_0 and $\zeta = \partial\nu/\partial T|_{T_0}$ is assumed constant. It is negative for silicon oil and glycerol.

The fluid motion is driven by surface stresses that arise due to the Marangoni effect. Within our model the surface tension σ is assumed to be a linear function of the temperature

$$\sigma = \sigma_0 - \gamma \left(T - T_0\right), \tag{3}$$

with σ_0 being the surface tension at temperature T_0. The coefficient $\gamma = -\partial\sigma/\partial T\,|_{T_0}$ is positive for most liquids. It can be negative, however, for some metal alloys.

2.2 Governing equations

Using Cartesian coordinates (x, y, z) the equation for mass, momentum, and energy conservation read

$$\frac{\partial U_j}{\partial x_j} = 0, \tag{4}$$

$$\rho_0 \frac{\partial U_i}{\partial t} + \rho_0 U_j \frac{\partial U_i}{\partial x_j} = \rho_0 \left[1 - \alpha \left(T - T_0\right)\right] F_i - \frac{\partial p}{\partial x_i} + \frac{\partial}{\partial x_j}\left[\mu\left(\frac{\partial U_i}{\partial x_j} + \frac{\partial U_j}{\partial x_i}\right)\right], \tag{5}$$

$$\rho_0 c \frac{\partial T}{\partial t} + \rho_0 c U_j \frac{\partial T}{\partial x_j} = k \frac{\partial^2 T}{\partial x_j^2}, \tag{6}$$

where U_i $(i = x, y, z)$ are the velocity components, $\mu = \rho_0\nu$ is the dynamic viscosity, k is the heat conductivity, and c is the specific heat. The pressure inside the fluid is denoted by p and $F_i = (0, 0, -g)$ is the gravity acceleration. Here Einstein's convention of summation over repeated indices is used.

2.3 Boundary conditions

At the rigid plate $(z = 0)$ the temperature is fixed $(T = T_0)$. No slip and no penetration boundary conditions are imposed for the velocity $(U_i = 0,\ i = x, y, z)$.

The perturbed free surface is given by

$$z_s(t, x, y) = d + \delta z_s(t, x, y). \tag{7}$$

Since δz_s is small compared to d, the boundary conditions at $z = z_s$ are linearized and written at $z = d$ by Taylor expansion. The kinematic condition reduces itself to the equation

$$U_z = \frac{\partial \delta z_s}{\partial t}\,. \tag{8}$$

Neglecting the gas motion above the layer, the velocity boundary conditions at the free surface are derived from the normal and tangential stress balance on the interface

$$-\left(p - p_g\right) + 2\mu \frac{\partial U_z}{\partial z} - \rho g \delta z_s = 2H\sigma, \tag{9}$$

$$\mu\left(\frac{\partial U_l}{\partial z} + \frac{\partial U_z}{\partial x_l}\right) = \frac{\partial \sigma}{\partial x_l}\ \ (l = x, y)\,. \tag{10}$$

In the above relations, p_g is the gas pressure, H is the mean curvature of the surface, given by $H = 1/2\nabla_s^2 z_s$, and ∇_s^2 is the two dimensional Laplacian operator $\partial^2/\partial^2 x + \partial^2/\partial^2 y$. The heat transfer balance subjected to Newton's law is of the form

$$\kappa \frac{\partial T}{\partial z} + h(T - T_g) = 0, \tag{11}$$

where h is the heat transfer coefficient between the liquid and gas phases and T_g the temperature of the ambient gas.

3 Linear stability analysis

The basic motionless state of the liquid layer ($\overline{\mathbf{U}} = (0,0,0)$) allows the following distributions for the temperature, the kinematic viscosity and the pressure fields

$$\begin{aligned} &\overline{T} = T_0 - \beta z, \overline{\nu} = \nu_0 - \zeta\beta z, \\ &\overline{p} = p_g + \rho_0 g\left[\frac{1}{2}\alpha\beta\left(z^2 - d^2\right) + (z-d)\right], \end{aligned} \tag{12}$$

where β is [9]:

$$\beta = \frac{h\left(T_0 - T_g\right)}{k + hd}\,. \tag{13}$$

For the stability analysis we consider

$$(\mathbf{U}, p, T) = (\overline{\mathbf{U}}, \overline{p}, \overline{T}) + (\mathbf{U}', p', T'), \tag{14}$$

where the perturbations $(\mathbf{U}', p', T')$ are functions of time and of all three spatial variables. The stability problem is investigated by means of a linear analysis. Accordingly, nonlinear terms are neglected.

In the dimensionless formulation, scales for length, time, velocity, temperature, and pressure have been taken to be d, d^2/χ, χ/d, βd, and $\rho_0\nu_0\chi/d^2$, respectively, where $\chi = k/\rho_0 c$ is the thermal diffusivity. Taking the curl of the momentum equations (5) by use of (4) and linearizing, the equations for the normal velocity component and pressure are obtained

$$Pr^{-1}\frac{\partial \nabla^2 U_Z}{\partial \tau} = Ra\nabla_s^2\theta + (1 - R_\nu Z)\nabla^4 U_Z - 2R_\nu \nabla^2 \frac{\partial U_Z}{\partial Z}, \tag{15}$$

$$\nabla^2 P = Ra\frac{\partial \theta}{\partial Z} - 2R_\nu \nabla^2 U_Z. \tag{16}$$

The corresponding linearized temperature equation is

$$\frac{\partial \theta}{\partial \tau} - U_Z = \nabla^2\theta. \tag{17}$$

Here $\nabla^2 = \partial^2/\partial X^2 + \partial^2/\partial Y^2 + \partial^2/\partial Z^2 = \nabla_s^2 + \partial^2/\partial Z^2$ is the Laplacian operator.

In equations (15–17) Z, τ, U_Z, P, and θ are dimensionless quantities. Three characteristic parameters have been introduced, namely

$$\begin{aligned} Pr &= \frac{\nu_0}{\chi}, && \text{Prandtl number,} \\ Ra &= \frac{g\alpha\beta d^4}{\nu_0\chi}, && \text{Rayleigh number,} \\ R_\nu &= \frac{\zeta\beta d}{\nu_0}, && \text{viscosity group.} \end{aligned} \tag{18}$$

The so-called viscosity group is a measure of the relative variation of the viscosity in the liquid volume. For example, the kinematic viscosity of silicon oil decreases from 10×10^{-2} cm^{2}s^{-1} to 6×10^{-2} cm^{2}s^{-1} for 10 cSt Silicon oil and from 50×10^{-2} cm^{2}s^{-1} to 28×10^{-2} cm^{2}s^{-1} for 50 cSt Silicon oil when the temperature increases from 25 ℃ to 60 ℃. These changes, which reach almost a factor of 2, correspond to $R_\nu = -0.5$.

At the rigid wall $Z = 0$, the boundary conditions are simply

$$U_Z = \frac{\partial U_Z}{\partial Z} = \theta = 0. \tag{19}$$

To present the normal stress balance (9) in the normal velocity terms, the surface Laplacian operator is applied on equation (9) and the term $(\nabla_s P)$ is eliminated by use of equations (4, 5). Taking the curl of equations (10) by use of equation (4) also allows the tangential stress balance to be expressed in normal velocity terms. Setting $\eta = \delta z_z/d$ for the surface deflection, gives

$$U_Z = \frac{\partial \eta}{\partial \tau}, \tag{20}$$

$$\begin{aligned} &Pr^{-1}\frac{\partial^2 U_Z}{\partial\tau\partial Z} - 3\left(1 - R_\nu\right)\frac{\partial \nabla_s U_Z}{\partial Z} - \left(1 - R_\nu\right)\frac{\partial^3 U_z}{\partial Z^3} \\ &- R_\nu\left(\nabla_s^2 U_Z - \frac{\partial^2 U_Z}{\partial Z^2}\right) - \frac{Bo}{Cr}\nabla_s^2\eta + \frac{1}{Cr}\nabla_s^4\eta = 0, \end{aligned} \tag{21}$$

$$\left(1 - R_\nu\right)\left(\nabla_s^2 U_Z - \frac{\partial^2 U_Z}{\partial Z^2}\right) = -Ma\nabla_s^2\left(\theta - \eta\right), \tag{22}$$

$$\frac{\partial \theta}{\partial Z} + Bi\left(\theta - \eta\right). \tag{23}$$

The dimensionless parameters Ma, Bo, Cr, Bi appearing in the boundary conditions are defined by

$$\begin{aligned} Ma &= \frac{\gamma\beta d^2}{\rho_0\nu_0\chi}, && \text{Marangoni number,} \\ Bo &= \frac{\rho_0 g d^2}{\sigma_0}, && \text{Bond number,} \\ Cr &= \frac{\rho_0\nu_0\chi}{\sigma_0 d}, && \text{crispation number,} \\ Bi &= \frac{hd}{k}, && \text{Biot number.} \end{aligned}$$

The effects of the surface deformability are measured by the Bond number and by the crispation number. While Bo estimates the effect on the modified static pressure by the gravity forces, Cr stands for the effect of the rigidity of the deformable surface. The Biot number models the heat transfer mechanism at the free surface. It represents the ratio of the liquid phase heat-transfer resistance and the gas phase transfer resistance. The value $Bi \to \infty$ corresponds to the conducting boundary and $Bi = 0$ to the insulating boundary.

By assumption, the free surface viscosity $\nu_s = \nu_0(1 - R_\nu)$ is taken to be a reference one the dimensionless parameters are redefined as

$$\begin{aligned}
\overline{Pr} &= \frac{\nu_s}{\chi} &&= Pr\,(1 - R_\nu)\\
\overline{Ra} &= \frac{g\alpha\beta d^4}{\nu_0\chi} &&= \frac{Ra}{(1 - R_\nu)}\\
\overline{R_\nu} &= \frac{\zeta\beta d}{\nu_s} &&= \frac{R_\nu}{(1 - R_\nu)}\\
\overline{Ma} &= \frac{\gamma\beta d^2}{\rho_0\nu_s\chi} &&= \frac{Ma}{(1 - R_\nu)}\\
\overline{Cr} &= \frac{\rho_0\nu_s\chi}{\sigma_0 d} &&= Cr\,(1 - R_\nu)\,.
\end{aligned}$$

The experimental set-up used in Bénard-Marangoni experiments could be outlined as a liquid layer confined between two rigid walls, but with a thin air gap between the free liquid surface and the upper plate. The upper plate is kept at a constant temperature while the lower rigid wall is heated. The temperature on the interface is not well-defined due to the heat transfer through the gas. The reference temperature, here, is the rigid wall temperature, considering the specificity of the experiments and in accordance with theoretical investigations.

For a given physical liquid layer with depth d, the only parameter that can be controlled is the temperature difference $T_0 - T_g = \beta d$. This is why, in practice, the three dimensionless parameters (Marangoni number, Rayleigh number, and the viscosity group) vary continuously with the applied temperature slope β through the layer.

Parameter $\Gamma_\nu = \gamma d/\rho_0\chi\zeta$ is defined only by the physical characteristics of the liquid layer, and is independent of the choice of the reference viscosity. So, $Ma = \Gamma_\nu R_\nu$ and the Boussinesq case is obtained at $\Gamma_\nu \to \infty$.

Even though the Rayleigh and the Marangoni numbers correspond to different instability mechanisms it is possible to introduce the parameter $\Gamma = \gamma/\rho_0\alpha g d^2$, that defines the ratio $Ma = \Gamma Ra$ (see, also Peréz-Garcia and Carneiro's work [14]). Pure thermocapillary instability is obtained at $\Gamma \to \infty$, while at $\Gamma = 0$ only the buoyancy instability is working.

In order to be within the limits of our model it is necessary that the applied temperature difference through the layer (βd) satisfy the inequality $\mid \beta d \mid \ll 1/\alpha$. In terms of the dimensionless parameters this reads as

$$Ra \ll Bo/Cr. \tag{24}$$

The condition is equivalent to those in [26] when surface tension is not considered. By use of the relation between Ma and Ra, in the case of the finite Γ (both instability mechanisms act simultaneously) (24) can be rewritten as

$$\mid Ma \mid \ll \mid \Gamma \mid Bo/Cr. \tag{25}$$

The general solution of equations (15, 17) with boundary conditions (19–23) is a superposition of the normal modes

$$(U_Z, \theta, \eta) = [W(Z), \Theta(Z), \delta_s]\, e^{\tilde{s}\tau} e^{i(\alpha_X X + \alpha_Y Y)} \tag{26}$$

where $\tilde{s} = s + i\omega$ is a complex growth rate with growth rate s and frequency ω, $\alpha^2 = \alpha_X^2 + \alpha_Y^2$ is the wave number, and W, Θ, δ_s the amplitudes. Here marginal or neutral stability is under investigation, so one gets $s = 0$.

Introducing (26) in equations (15, 17) the following set of linearized differential equations is obtained for the normal velocity and the temperature amplitudes

$$\begin{aligned}
&\left(D^2 - \alpha^2\right)^2 W - i\omega Pr^{-1}\left(D^2 - \alpha^2\right) W\\
&\quad - R_\nu\left[2\left(D^2 - \alpha^2\right) DW + Z\left(D^2 - \alpha^2\right)^2 W\right] = Ra\alpha^2\Theta,
\end{aligned} \tag{27}$$

$$\left(D^2 - \alpha^2 - i\omega\right)\Theta = -W, \tag{28}$$

where D stands for d/dZ. The corresponding boundary conditions are

$$W = DW = \Theta = 0, \quad \text{at } Z = 0 \tag{29}$$

$$\left.\begin{aligned}
W - i\omega\delta_s &= 0\\
Pr^{-1} i\omega D^2 W &\\
+3\alpha^2(1 - R_\nu) DW - (1 - R_\nu) D^3 W &\\
+R_\nu\left(D^2 + \alpha^2\right) W + \tfrac{1}{Cr}\alpha^2\left(\alpha^2 + Bo\right)\delta_s &= 0\\
(1 - R_\nu)\left(D^2 + \alpha^2\right) W &= -Ma\alpha^2(\Theta - \delta_s)\\
D\Theta + Bi\,(\Theta - \delta_s) &= 0
\end{aligned}\right\} \quad \text{at } Z = 1. \tag{30}$$

Equations (27,28) can be reduced to a single sixth order equation for the Θ variable alone

$$\begin{aligned}
&\left(D^2 - \alpha^2 q^2\right)\left(D^2 - \alpha^2 r^2\right)\left(D^2 - \alpha^2\right)\Theta - R_\nu\left(D^2 - \alpha^2 q^2\right)\\
&\times\left(D^2 - \alpha^2\right)\left[2D\Theta + Z\left(D^2 - \alpha^2\right)\Theta\right] = -\alpha^2 Ra\Theta,
\end{aligned} \tag{31}$$

where $r^2 = 1 + i\omega/\alpha^2 Pr$ and $q^2 = 1 + i\omega/\alpha^2$. The relevant boundary conditions are also rewritten in terms of Θ.

The eigenvalue problem defined by equation (31) and boundary conditions (29, 30) is solved by searching for the solution in the form of a series expansion in Z

$$\Theta(z) = \sum_{j=0}^{N} E_j\, Z^j. \tag{32}$$

Table 1. Physical data for different types of silicon oil and corresponding dimensionless parameters Γ_ν, Γ, Pr, Bo, and Cr at $d = 0.1$ cm.

Silicon oil	$47\,V\,5$	$47\,V\,10$	$47\,V\,20$	$47\,V\,100$
$\rho\,[\mathrm{g/cm^3}]$	0.910	0.930	0.950	0.965
$\nu \times 10^2\,[\mathrm{cm^2/s}]$	5	10	20	100
$\chi \times 10^4\,[\mathrm{cm^2/s}]$	6.69	8.60	9.17	11.25
$\alpha \times 10^3\,[^\circ\mathrm{C}^{-1}]$	1.0	1.08	1.07	0.945
$\sigma\,[\mathrm{dyn/cm}]$	19.7	20.1	20.6	20.9
$\gamma\,[\mathrm{dyn/cm}\ ^\circ\mathrm{C}]$	0.068	0.069	0.06	0.05
Γ_ν	$-20\,576$	$-7\,549$	$-2\,940$	-358
Γ	7.3	7.0	6.0	5.6
Pr	75	116	218	889
Bo	0.45	0.45	0.45	0.45
Cr	1.545×10^{-5}	3.979×10^{-5}	0.845×10^{-4}	5.19×10^{-4}

Using rigid boundary conditions (29), all expansion coefficients E_j are determined with three arbitrary constants chosen to be E_1, E_4, E_5 taking $E_0 = 0$, $E_2 = 0$, $E_3 = E_1(\alpha^2 + i\omega)$ and

$$E_6 = -\frac{\left(\sum_{i=0}^{5} a_{0,i}\,E_i\right)}{a_{0,6}}, \qquad E_7 = -\frac{\left(\sum_{i=0}^{6} a_{1,i}\,E_i\right)}{a_{1,7}},$$

$$E_8 = -\frac{\left(\sum_{i=0}^{7} a_{2,i}\,E_i\right)}{a_{2,8}}, \qquad E_9 = -\frac{\left(\sum_{i=0}^{8} a_{3,i}\,E_i\right)}{a_{3,9}},$$

$$E_{10} = -\frac{\left(\sum_{i=0}^{9} a_{4,i}\,E_i\right)}{a_{4,10}}, \qquad E_{11} = -\frac{\left(\sum_{i=0}^{10} a_{5,i}\,E_i\right)}{a_{5,11}},$$

$$E_{j+6} = \frac{\left(\sum_{j=0}^{11} a_{j,j-6+i}E_i\right)}{a_{+6}} \qquad \text{for } j \geq 6.$$

The free boundary conditions (30) are introduced into the three-constant solution for Θ.

The condition for the existence of a nontrivial solution (the characteristic determinant of the resulting homogeneous linear set of equations must be zero) determines the stability criteria

$$Ma = F(\alpha,\, \omega,\, Pr,\, Bo,\, Cr,\, Ra,\, R_\nu, Bi\,), \tag{33}$$

where F is a real valued function of the parameters in parentheses. The stationary stability curve is obtained under the condition $\omega = 0$, while $\omega \neq 0$ corresponds to the oscillatory convective motion. As to the oscillatory case, it is clear that for arbitrary values of the enumerated parameters, the value of Ma will generally be complex ($Ma = Ma_r + i\,Ma_i$). The solution of the problem is only reasonable for a real value of Ma. A numerical search has been conducted to find the value of ω that makes the imaginary part of Ma vanish. The numerical accuracy, of the order of 10^{-4}, is achieved by increasing the number N of expansion coefficients.

4 Results and comments

Our investigation is concerned with silicon oil as it is the liquid mostly used in the Bénard-Marangoni experiments and its viscosity is strongly temperature dependent. The available physical data for different types of silicon oil and calculated dimensionless parameters Γ_ν, Γ, Pr, Bo, and Cr for a liquid layer with depth $d = 0.1$ cm are presented in Table 1, while the values of the dimensionless parameters Γ_ν, Γ, the crispation, and the Bond number for the quoted experiments [3–6] are given in Table 2. The Bond number and the parameter Γ are influenced mainly by the depth of the liquid, whereas the parameter Γ_ν, the Prandtl number and the crispation number are strongly affected by the type of silicon oil, and their values drastically change with an increase of the kinematic viscosity. In all cases investigated the free surface is assumed to be insulated, *e.g.* $Bi = 0$. The estimated value of Bi for the quoted experiments is less than 1 and having this into account leads to a slight increase of the critical parameters.

Detailed calculations have been carried out for the viscosity group which varies between -0.5 and 0.5. The sign of the viscosity group depends on the type of liquid (whether the viscosity is an increasing or a decreasing function of the temperature) as well as on the type of heating (from below or from above). The more relevant physical parameter accounting for viscosity effects is Γ_ν defined only by means of the thermophysical characteristics of the liquid. For a liquid such as silicon oil it is negative and the sign of parameters Ma and R_ν is always opposite.

Reliable calculations for the convective threshold available in the literature are used to validate the code. In the limit $R_\nu \to 0$, neglecting the gravity ($Ra = 0$), but considering the surface deformability ($Cr \neq 0$) Takashima's results [9,10] for stationary and oscillatory convection are found. An additional check is made by comparing our results with linear stability boundaries given by Gouesbet *et al.* [13] and Pérez-Garcia and Carneiro [14] when $Ra \neq 0$,

Table 2. Values of the parameter Γ_ν, Γ, and Cr for the Bénard-Marangoni experiments.

		d [cm]	Γ_ν	Γ	Cr	Bo
Koshmieder and	100 cSt	0.3	−1 100	0.6	1.8×10^{-4}	4.41
Switzer [3]		0.19	−697	1.5	2.9×10^{-4}	1.77
	50 cSt	0.19	−1 444	1.3	2.8×10^{-4}	1.85
		0.12	−912	3.3	4.4×10^{-4}	0.74
Nitschke and Thess [4]	10 cSt	0.155	−7 511	2.9	2.6×10^{-5}	1.08
Schatz *et al.* [5]	7.1 cSt	0.0419	−4 249	38.9	6.8×10^{-5}	0.079
VanHook *et al.* [6]	10.2 cSt	0.005	−321	2 952	9.7×10^{-4}	0.001
		0.025	−1 605	118	1.9×10^{-4}	0.028

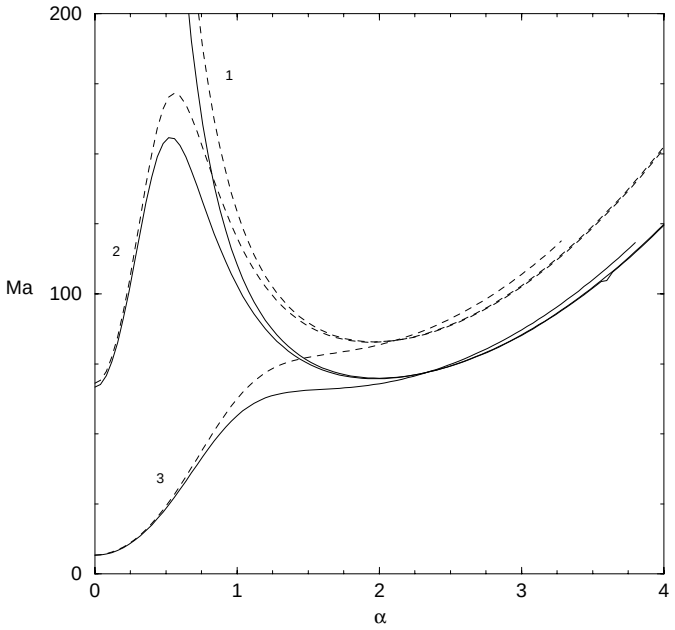

Fig. 1. Marginal stability curves Ma *vs.* α, for $Bo = 0.1$, $Bi = 0$, $\Gamma = 0.8$ and different values of the crispation number: $Cr = 0$ (label 1); $Cr = 10^{-3}$ (label 2); $Cr = 10^{-2}$ (label 3). Solid curves refer to $R_\nu = 0$ and dashed curves to $R_\nu = -0.3$.

$Cr \neq 0$, and $R_\nu = 0$. Table 3 shows perfect agreement between the quoted results and our own. A severe test of the effects of viscosity is provided by comparison with Selak and Lebon's results [22] when $Cr = 0$, and $Ra \neq 0$, and with our previous data [24] at $Ra = 0$, $Cr \neq 0$. These various favourable tests strongly validate our numerical results.

Table 3. Critical values of the stationary Marangoni numbers Ma_{sc}, oscillatory Marangoni number Ma_{oc} and corresponding wave numbers and wave frequencies at $Ra = Bi = 0$, $Bo = 0.1$ and $Pr = 1$.

R_ν	Cr	α_{sc}	Ma_{sc}	α_{oc}	ω_{oc}	Ma_{oc}
−0.3	0	1.97	94.875	-	-	-
0	0	1.99	79.607	-	-	-
0.3	0	2.03	63.609	-	-	-
−0.3	10^{-1}	0	0.681	0.28	7.05	−1 198.51
0	10^{-1}	0	0.667	0.28	6.59	−1 015.98
0.3	10^{-1}	0	0.647	0.27	6.10	−870.01
−0.3	10^{-2}	0	6.813	0.27	7.22	−1 229.01
0	10^{-2}	0	6.667	0.28	6.76	−1 043.97
0.3	10^{-2}	0	6.471	0.28	6.27	−893.27
−0.3	10^{-3}	0	68.135	0.34	9.84	−1 373.72
0	10^{-3}	0	66.667	0.59	16.62	−1 075.91
0.3	10^{-3}	1.99	62.822	0.60	15.62	−743.72
−0.3	10^{-4}	1.96	94.735	0.34	17.39	−2 140.84
0	10^{-4}	1.99	79.499	0.34	16.55	−1 895.65
0.3	10^{-4}	2.03	63.531	0.32	15.50	−1 659.62
−0.3	10^{-5}	1.97	94.861	0.18	21.79	−9 129.65
0	10^{-5}	1.99	79.596	0.18	20.72	−8 552.32
0.3	10^{-5}	2.03	63.601	0.17	19.59	−7 982.13
−0.3	10^{-6}	1.97	94.873	0.02	26.21	−65 260.21
0	10^{-6}	1.99	79.606	0.08	26.19	−62 785.51
0.3	10^{-6}	2.03	63.608	0.08	24.55	−60 462.71

4.1 Stationary convection

It is well-known that the Prandtl number does not influence the stationary mode, so the critical value of the stationary Marangoni number Ma_{sc} does not vary with Pr.

In Figure 1 typical stationary marginal stability curves $Ma(\alpha)$ are plotted for $\Gamma = 0.8$ and several values of the crispation number ($Cr = 0;\ 10^{-2}\ ; 10^{-3}$). Solid lines correspond to the constant viscosity ($R_\nu = 0$), while dashed lines represent the temperature-dependent viscosity ($R_\nu = -0.3$). When the free surface is non-deformable the curves, labelled by 1, have a minimum at a non-zero value of the wave number. An increase of parameter R_ν causes a decrease of the critical value of the stationary Marangoni number Ma_{sc} and a slight increase of the corresponding wave number α_{sc} (see, also Tab. 3). For pure thermocapillary convection, the relative deviation of Ma_{sc} due to the variable-viscosity effect is 19.1% at $R_\nu = -0.3$.

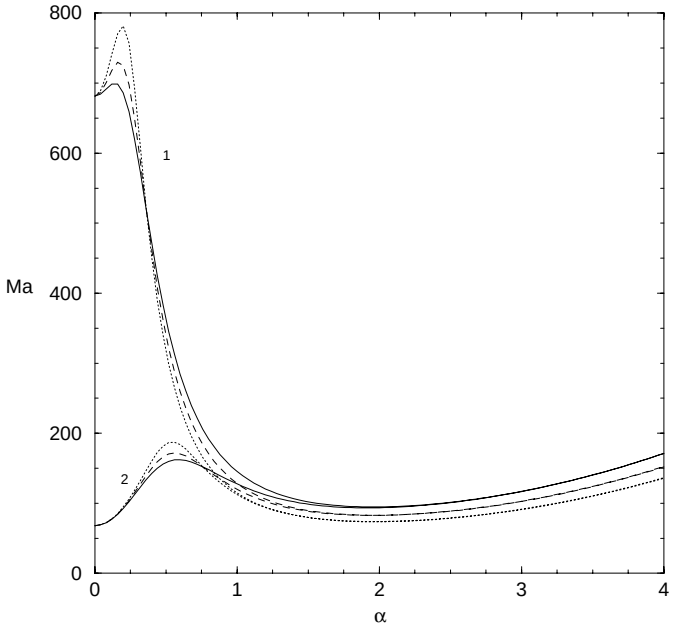

Fig. 2. Marginal stability curves Ma *vs.* α, for $Bo = 0.1$, $R_\nu = -0.3$, $Bi = 0$ and for two values of the crispation number: $Cr = 10^{-4}$ (label 1); $Cr = 10^{-3}$ (label 2). Solid curves refer to pure thermocapillary case $\Gamma \to \infty$, dashed curves to $\Gamma = 0.8$ and dotted to $\Gamma = 0.4$.

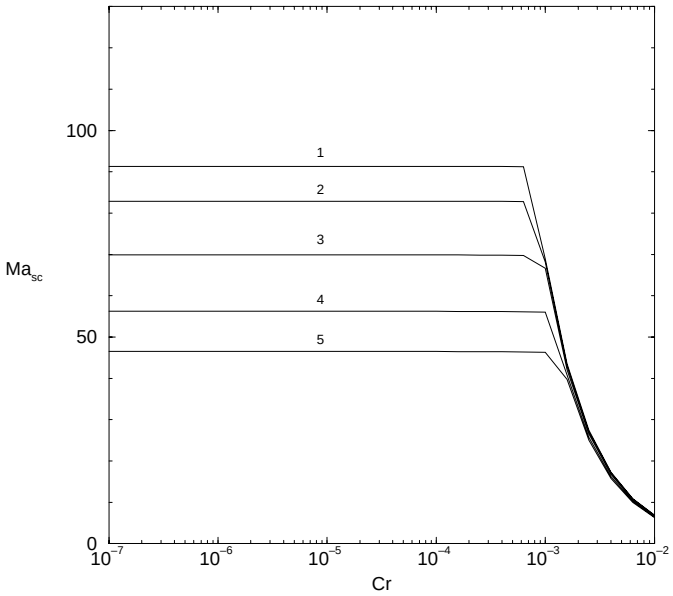

Fig. 3. Critical Marangoni number Ma_{sc} *vs.* the crispation number for $Bo = 0.1$, $Bi = 0$, $\Gamma = 0.8$ and various values of the viscosity group: $R_\nu = -0.5$ (label 1); $R_\nu = -0.3$ (label 2); $R_\nu = 0$ (label 3); $R_\nu = 0.3$ (label 4); $R_\nu = 0.5$ (label 5).

When surface deformability is considered ($Cr \neq 0$) the stationary neutral curve has two local minima, one located at $\alpha_c = 0$ and the other at α_c approximately equal to 2. The minimum located at $\alpha_c = 0$ is not very sensitive to the variation of R_ν and it is mainly determined by the surface deformability. At $R_\nu = 0$ in the pure thermocapillary case even the value of the local minimum is reduced to

$$Ma_0 = \frac{2Bo(1+Bi)}{Cr}\,.$$

When Cr becomes large the zero-mode becomes the most dangerous one and the long-wavelength instability sets in as a primary one. In contrast, for small values of Cr the global minimum occurs at $\alpha_c = 2$ and instability will start under the form of polygonal cells. At some transient value of the crispation number, the neutral curve has two equal local minima (one at zero wave number and the other at non-zero wave number) and the corresponding two spatial modes can coexist. The neutral curve around the second minimum is almost insensitive to the surface deformation, but it is influenced by the variable-viscosity effects (see, also Tab. 3).

The parameter Γ is the only relevant physical parameter accounting for the relative importance of thermocapillary and buoyant instability mechanisms. In order to show the contributions of buoyancy force, in Figure 2 we have represented Ma as a function of α for several values of the parameter Γ: pure thermocapillary instability mechanism ($\Gamma \to \infty$), $\Gamma = 0.8$ and $\Gamma = 0.4$. The Bond number is equal to 0.1, and the crispation number takes two values 10^{-4} and 10^{-3}. Solid lines refer to the pure thermocapillary mechanism, dashed lines to $\Gamma = 0.8$ and dotted ones to $\Gamma = 0.4$. For small wave numbers, the buoyancy force leads to an increase of the Marangoni number, but the local minimum at $\alpha = 0$ is independent of Γ and consequently of Ra. One may conclude that below some depth of the liquid layer determined by the crispation number at which the two local minima coincide, stationary convection is insensitive to the buoyancy instability mechanism. For wave numbers of order one and greater it causes a decrease of Ma, so that, for a certain value of Cr below which the global minimum coincides with the second one, the buoyancy force destabilizes the liquid system.

The dependence of a variable viscosity on the critical Marangoni number is reported in Figure 3 at $\Gamma = 0.8$, $Bo = 0.1$ and several values of the viscosity group $R_\nu = -0.5\,; -0.3\,; 0\,; 0.3\,; 0.5$. The buoyancy force enhances the instability, leading to a decrease of the convective threshold, to be compared with the pure thermocapillary study [24]. For sufficiently high values of the crispation number ($Cr > 10^{-3}$), the influence of a variable viscosity is minute. When the kinematic viscosity at the hot wall is taken to be the reference viscosity, a negative (positive) value of R_ν stabilizes (destabilizes) the layer.

The Marangoni number and viscosity group are linked through the parameter Γ_ν which is independent of the temperature difference. So, a fixed value of Γ_ν corresponds to a pair of critical parameters Ma_{sc} and R_ν^c. For the layer of 100 cSt silicon oil with depth varing from 0.055 cm to 0.7 cm, the parameter Γ_ν decreases from -200 to -2500. In Table 4 the parameter R_ν^c, the critical wave number, and the value of the convective threshold are presented for a non-deformable case ($Cr = Bo = 0$) and various values of Γ_ν. The increase of Γ_ν from $-\infty$ to -200 leads to an increase of the convective threshold from 79.607 to 106.309, while the critical wave number is weakly sensitive to

Table 4. Critical values of the stationary Marangoni numbers Ma_{sc}, wave numbers α_{sc}, and corresponding values of the viscosity group R_ν^c at different Γ_ν.

Γ_ν	R_ν^c	α_{sc}	Ma_{sc}
-200	-0.53	1.95	106.309
-300	-0.33	1.97	95.845
-400	-0.23	1.97	91.268
-500	-0.18	1.98	88.704
-700	-0.12	1.98	85.923
-900	-0.09	1.98	84.443
-1500	-0.05	1.99	82.445
-2500	-0.03	1.99	81.289
$-\infty$	0	1.99	79.607

these variations. The effect of a variable viscosity vanishes for $\Gamma_\nu < -2500$.

The results, given above, presenting the influence of deformability and viscosity on the convective threshold give a better understanding of the recent experiments [3–6]. Since $\Gamma_\nu < -2500$ (see, Tab. 2) the effect of nonzero R_ν is negligible for the experiments of Nitschke and Thess [4], and Schatz *et al.* [5]. VanHook *et al.* [6] considered very a thin liquid layer where instability sets in as a long-wavelength insensitive to a variable viscosity effect.

The values of Γ_ν and Γ are easily obtained from the parameter values tabulated in each experiment [3]. Since the reference viscosity in Koschmieder and Switzer's experiments is given at the temperature of the cold wall the modified critical Marangoni number $\overline{Ma_{sc}}$ is used here. In order to better distinguish between the the effects of the variable viscosity and the buoyancy, the critical Marangoni number ($\overline{Ma_{sc}^*}$) calculated at the same value of the parameter Γ_ν, but at the given Rayleigh number instead of at the given Γ, is also determined. The critical Marangoni number predicted by Nield's theoretical approach is noted by Ma_n. The values of these three critical Marangoni numbers and corresponding ratios to the experimentally measured Marangoni number (Ma_{ce}) are given in Table 5. For the first experiment only with a 0.3 cm layer depth used here model slightly increases the shift between the theoretically predicted and the experimentally measured threshold. In all other cases investigated the ratio increases from 0.82 to 0.86 for 0.19 cm 100 cSt silicon oil, from 0.97 to 1.00 for 0.19 cm 50 cSt silicon oil, and from 0.79 to 0.82 for 0.12 cm 50 cSt silicon oil. The shift between $Ma_{ce}/\overline{Ma_{sc}}$ and $Ma_{ce}/\overline{Ma_{sc}^*}$ is less than 0.01. So, one may conclude that the use of a variable-viscosity model provides a theoretical approach closer to the experimental data.

4.2 Oscillatory convection

While Takashima [10] proves the existence of oscillatory convection in a liquid layer with a deformable upper surface and a purely thermocapillary mechanism, Benguria and Depassier [26] show that the oscillatory convection can also arise from the purely buoyancy mechanism alone. The effects of the simultaneous action of thermocapillary and buoyancy mechanisms are investigated in the work of Gouesbet *et al.* [13] in the region $Ma, Ra < 0$ and of Pérez-Garcia and Carneiro [14] in the region $Ma < 0, Ra > 0$. The parameter Γ, defining the ratio between Ma and Ra is positive for most liquids. It can be negative, however, for some metal alloys. Both cases treat $Bo > 0$. A layer of liquid with positive Γ above a cold wall is studied in the first case, while the layer of liquid with negative Γ above a heated wall is considered in the second case.

Numerically it has been found that the neutral oscillatory Marangoni numbers are always negative, which coincides with Takashima's results [10] in the pure thermocapillary case, as well as with those of Gouesbet *et al.* [13] and Pérez-Garcia and Carneiro's [14] in the case of the simultaneous action of both instability mechanisms.

The absolute threshold shift introduced by a variable viscosity is stronger for the oscillatory than for the stationary convection (see, Tab. 3). However, the relative deviations, for example, at $Cr = 10^{-4}$ are: 13% for $R_\nu = -0.3$ and 12.5% for $R_\nu = 0.3$ for the oscillatory convection, and 19% for $R_\nu = -0.3$ and 20% for $R_\nu = 0.3$ in the the stationary convection.

Since our investigation is devoted to silicon oil with a positive value of the parameter Γ, here, we aim to extend the stability analysis of Gouesbet *et al.* [13]. As has already been mentioned, such a liquid has opposite sign for the Marangoni number and the viscosity group. Positive values of R_ν are physically relevant when the stability criteria for a cooling rigid wall (negative values of the oscillatory Marangoni number) are under investigation.

In the pure thermocapillary case ($Ra = 0$) the liquid layer stability increases with a decrease of Cr, see Table 3. But dependending on the values of Pr, Bo and Bi there is an interval of the crispation number where the critical Marangoni number is a decreasing function of Cr. For instance, at $Pr = 1$, $Bo = 0.1$ and $Bi = 0$ it is $[10^{-3}, 10^{-4}]$. This coincides also with the results of Takashima [10] and Gouesbet *et al.* [13]. As in the stationary case, the oscillatory neutral curve can also have two minima. The situation when these two minima coincide corresponds to a jump of the critical wave numbers, accompanied by a jump of the frequencies and by a discontinuity in the slope of $Ma_c(Ra_c)$ curves. The conditions under which oscillatory and stationary modes can coexist simultaneously are determined by Pérez-Garcia and Carneiro [14]. To ensure that we remain within the limits of our model, we have restricted the results obtained using equation (24). Due to this reason we have not paid attention here to the problem of coexistence of these minima.

In Figure 4a, 4b the neutral curves are presented in the (Ma_c, Ra_c) – plane at $R_\nu = 0$; 0.3 respectively. The results are obtained at $Bo = 0.1$, $Pr = 1$, $Bi = 0$ and several values of the crispation number: $Cr = 0.0015$; 0.001; 0.0005. Solid lines refer to stationary convection and dashed ones to oscillatory convection.

Table 5. Relative deviation of the theoretical predicted convective threshold from the experimental data.

	d [cm]	Ma_{ce}	Γ_ν	Γ	$\overline{Ma_{sc}}$	$\frac{Ma_{ce}}{\overline{Ma_{sc}}}$	Ra	$\overline{Ma^*_{sc}}$	$\frac{Ma_{ce}}{\overline{Ma^*_{sc}}}$	Ma_n	$\frac{Ma_{ce}}{Ma_n}$
100 cSt	0.3	71.0	−1 100	0.6	65.8	1.08	115	66.8	1.08	66.8	1.06
	0.19	61.8	−697	1.5	71.5	0.86	40	72.6	0.85	75.2	0.82
50 cSt	0.19	72.1	−1 444	1.3	72.1	1.00	54	72.5	0.99	73.6	0.97
	0.12	61.4	−912	3.3	74.8	0.82	18	75.4	0.81	77.6	0.79

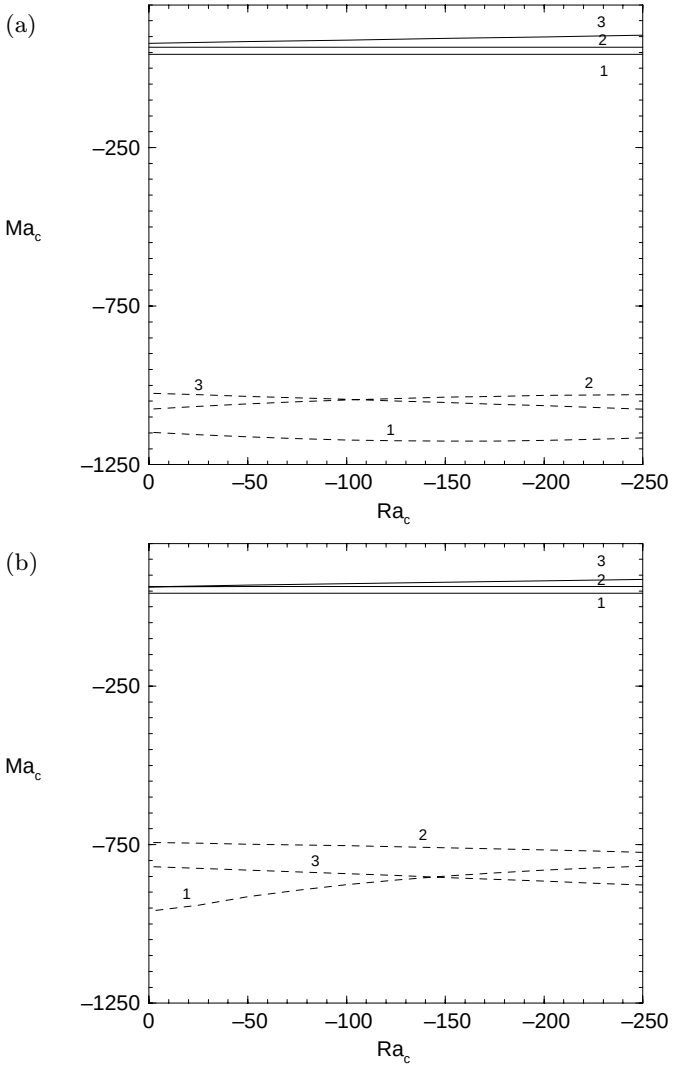

Fig. 4. Critical Marangoni number Ma_c *vs.* the Rayleigh number for $Bo = 0.1$, $Pr = 1$, $Bi = 0$ and various values of the crispation number: $Cr = 0.0015$ (label 1); $Cr = 0.001$ (label 2); $Cr = 0.0005$ (label 3). Solid curves refer to stationary critical Marangoni number Ma_{sc} and dashed ones to oscillatory Marangoni number Ma_{oc}. The viscosity group is equal to 0 and 0.3 on a, and b, respectively.

The region between solid and dashed lines corresponds to the stable case. The viscosity group is equal to 0 and 0.3 on a, and b, respectively.

As is seen from the graphics, the temperature-dependent viscosity destabilises the liquid system but the values

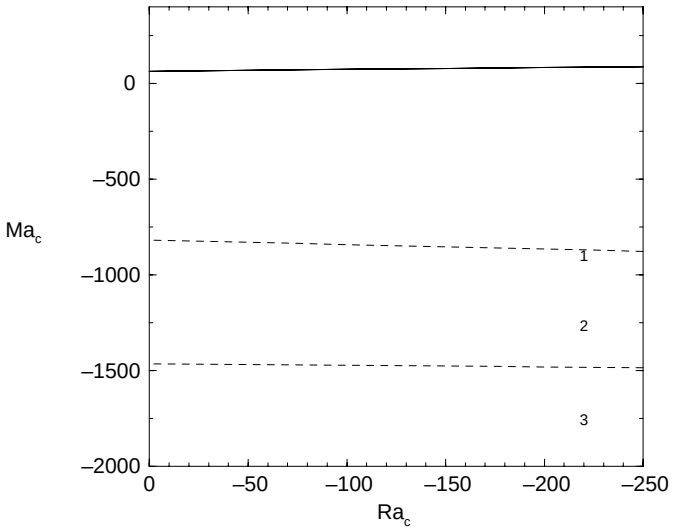

Fig. 5. Critical Marangoni number Ma_c *vs.* the Rayleigh number for $Bo = 0.1$, $Cr = 0.0005$, $R_\nu = 0.3$, $Bi = 0$ and various values of the Prandtl number: $Pr = 1$ (label 1); $Pr = 2$ (label 2); $Pr = 3$ (label 3). Solid curves refer to stationary critical Marangoni number Ma_{sc} and dashed ones to oscillatory Marangoni number Ma_{oc}.

are not qualitatively different from the Boussinesq values. Only the behaviour of Ma_c at $Ra_c = 0$ is different because the interval of the crispation numbers where Ma_c is a decreasing function of Cr depends also on R_ν.

In the usual case with positive Γ when $T_o < T_g$ ($Ma_c = Ma_{oc} < 0$) the instability sets in as oscillations. From the results presented in Figure 4 one may conclude that the instability can occur as an oscillatory motion when the temperature of the solid wall is lower than that of the ambient gas.

In order to give an idea of how the Prandtl number influences the layer stability, in Figure 5 the critical Marangoni number Ma_c is plotted against the Rayleigh number for $Cr = 0.0005$, $Bo = 0.1$, $R_\nu = 0.3$, $Bi = 0$ and various values of the Prandtl number: $Pr = 1$; 2; 3. As can be seen, the stability of the layer is strongly amplified by the increase of Pr. An increase of the Prandtl number from 1 to 2 causes decrease of Ma_{oc} of almost a factor of two.

The critical Marangoni number Ma_c *versus* the Rayleigh number for $Cr = 0.0005$, $R_\nu = 0.3$, $Pr = 1$, $Bi = 0$ and various values of the Bond number: $Bo = 0.1;\ 0.5\ ;1$ is given in Figure 6. An increase of the overstatic pressure

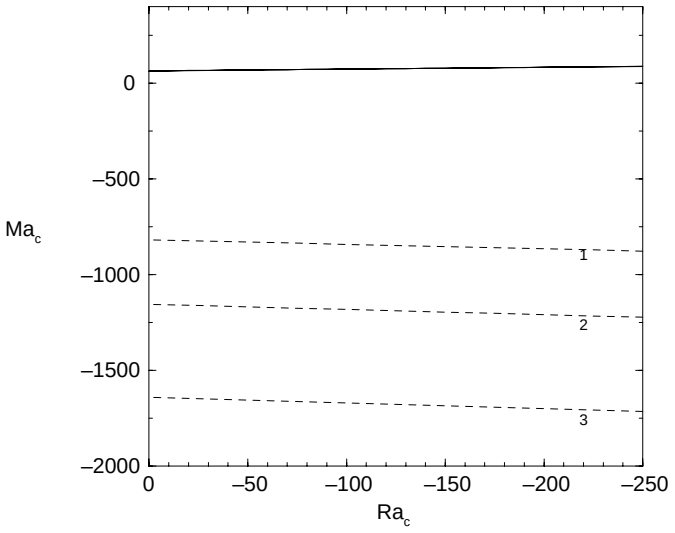

Fig. 6. Critical Marangoni number Ma_c *vs.* the Rayleigh number for $Cr = 0.0005$, $R_\nu = 20.3$, $Pr = 1$, $Bi = 0$ and various values of the Bond number: $Bo = 0.1$ (label 1); $Bo = 0.5$ (label 2); $Bo = 1$ (label 3). Solid curves refer to stationary critical Marangoni number Ma_{sc} and dashed ones to oscillatory Marangoni number Ma_{oc}.

(the Bond number), taking place with an increase of the liquid depth, also stabilises the liquid system.

Figures 4–6 give an idea of how the most physically relevant parameters influence the oscillatory instability. Since the Prandtl number strongly enhances the layer stability we direct our interest to 0.65 cSt Silicon oil ($Pr = 8.4$). For such a liquid the parameter Γ_ν lies in the interval $[-15\,000,\ -150\,000]$ for a liquid depth between 0.005 cm and 0.05 cm. For $d = 0.05$ cm the corresponding values of crispation and Bond number are $Cr = 0.0001$ and $Bo = 0.1$.

In Table 6 the values of Γ_ν and the corresponding critical values of the viscosity group, the wave number, the frequency, and oscillatory Marangoni number are tabulated for two different Prandtl numbers ($Pr = 1$, and $Pr = 8.4$) at $Cr = 0.0001$ and $Bo = 0.1$. The preceding analysis indicates that a variable viscosity effect destabilizes the liquid system. This confirms what was expected as the negative Marangoni numbers obtained are equivalent to cooling of the rigid wall and the reference kinematic viscosity used is greater than the mean viscosity.

In spite of the destabilising effect of a variable viscosity, all the determined critical oscillatory Marangoni numbers remain large an order of 10^3 which is related to a critical temperature difference between 50 ° and 100 ° that is impossible to obtain physically for such a thin liquid layer.

Table 6. Critical values of the oscillatory Marangoni numbers Ma_{oc}, wave numbers α_{oc}, wave frequencies ω_{oc}, and corresponding values of the viscosity group R_ν^c at different Γ_ν.

$Pr = 1$				
Γ_ν	R_ν^c	α_{oc}	ω_{oc}	Ma_{oc}
−2 500	0.58	0.31	14.30	−1 447.39
−3 000	0.50	0.31	14.67	−1 505.53
−5 000	0.33	0.32	15.41	−1 638.23
−7 000	0.24	0.33	15.73	−1 703.36
−10 000	0.18	0.33	15.99	−1 756.35
−15 000	0.12	0.33	16.16	−1 800.16
−20 000	0.09	0.33	16.21	−1 823.02
−25 000	0.07	0.33	16.21	−1 837.07
−30 000	0.06	0.33	16.34	−1 846.48
$-\infty$	0	0.33	16.53	−1 895.65

$Pr = 8.4$				
Γ_ν	R_ν^c	α_{oc}	ω_{oc}	Ma_{oc}
−15 000	0.51	0.44	80.94	−7 700.58
−20 000	0.42	0.44	82.22	−8 495.06
−30 000	0.32	0.44	83.71	−9 511.52
−40 000	0.25	0.44	84.19	−10 136.94
−50 000	0.21	0.44	84.71	−10 564.60
−60 000	0.18	0.44	84.73	−10 872.45
−80 000	0.14	0.44	84.83	−11 290.90
−100 000	0.12	0.44	85.25	−11 561.05
−150 000	0.08	0.43	85.21	−11 946.88
$-\infty$	0	0.43	85.25	−12 816.50

4.3 Conclusion

The linear stability properties of a liquid layer with variable viscosity and a deformable free surface are studied under the simultaneous action of surface-tension and buoyancy-driven instability mechanisms. The investigation is particularly focussed on the role of the crispation number and it is shown that an increase of this parameter abruptly changes the value of the critical wave number. Stationary convection occurs with finite or infinite wavelength. Numerical computations prove that considering the variable viscosity effects leads only to a quantitative change in the stability parameters. When the rigid wall is cold it is found that oscillatory instability sets in for most liquids with decreasing surface tension with temperature. It is demonstrated that the increase of the Prandtl number leads to a considerable stabilization of the liquid system.

The authors gratefully acknowledge the constructive comments and criticisms of the referees which have contributed to the improvement of the present article. This research is supported by the Bulgarian National Foundation for Scientific Research under contract TN-402/94 and by the Program for scientific cooperation between the Bulgarian Academy of Sciences and the CNRS – France.

References

1. J.R.A. Pearson, J. Fluid Mech. **4**, 489 (1958).
2. D.A. Nield, J. Fluid Mech. **9**, 341 (1964).
3. E.L. Koschmieder, D.W. Switzer, J. Fluid Mech. **240**, 533 (1992).
4. E. Nitschke, A. Thess, Phys. Rev. E. **52**, 5772 (1995).
5. M.F. Schatz *et al.*, Phys. Rev. Lett. **75**, 1938 (1995).
6. S.J. VanHook *et al.*, Phys. Rev. Lett. **75**, 4397 (1995).
7. L.E. Scriven, C.V. Sternling, J. Fluid Mech. **19**, 321 (1964).
8. K.A. Smith, J. Fluid Mech. **24**, 401 (1966).
9. M. Takashima, J. Phys. Soc. Jap. **50**, 2745 (1981).
10. M. Takashima, J. Phys. Soc. Jap. **50**, 2751 (1981).
11. J. Castillo, M. Velarde, J. Fluid Mech. **125**, 463 (1982).
12. R.D. Benguria, M.C. Depassier, Phys. Fluids A **1**, 1123 (1989).
13. G. Gouesbet *et al.*, Phys. Fluids A **2**, 903 (1990).
14. C. Pérez-Garcia, G. Carneiro, Phys. Fluids A **3**, 292 (1991).
15. E. Palm, J. Fluid Mech. **8**, 183 (1960).
16. K.C. Stengel, D.S. Oliver, J.R. Booker, J. Fluid Mech. **120**, 411 (1982).
17. D.B. White, J. Fluid Mech. **191**, 247 (1988).
18. M. Ogawa, G. Schubert, A. Zebib, J. Fluid Mech. **233**, 299 (1991).
19. C.Q. Hoard, C.R. Robertson, A. Acrivos, Int. J. Heat Mass Transfer **13**, 849 (1970).
20. A. Cloot, G. Lebon, PCH Phys. Chem. Hydrodyn. **6**, 453 (1985).
21. G. Lebon, in *Physicochemical Hydrodynamics. Interfacial Phenomena*, edited by M.G. Velarde (1988), p. 253.
22. R. Selak, J. Phys. II France **3**, 1185 (1993).
23. R. Selak, G. Lebon, Int. J. Heat Mass Transfer **40**, 785 (1997).
24. Zh. Kozhoukharova, C. Rozé, G. Lebon, Microgravity Sci. Technol. **8** 249 (1995).
25. S. Slavtchev, V. Ouzunov, Microgravity Q. **4**, 33 (1994).
26. R.D. Benguria, M.C. Depassier, Phys. Fluids **30**, 1678 (1987).